Journal of Electrochemistry

Volume 23 | Issue 4

2017-08-25

Effects of surface modification modes on proton-over-vanadium ion selectivity of Nafion®membrane for application in vanadium redox flow battery

Qing-long TAN

Hai-ning WANG

Shan-fu LU

Da-wei LIANG

Chun-xiao WU

Yan XIANG

DOI: 10.13208/j.electrochem.160307 **Artical ID**:1006-3471(2017)04-0409-11
Cite this: *J. Electrochem.* **2017**, *23*(4): 409-419 **Http**://electrochem.xmu.edu.cn

Effects of Surface Modification Modes on Proton-over-Vanadium Ion Selectivity of Nafion® Membrane for Application in Vanadium Redox Flow Battery

TAN Qing-long, WANG Hai-ning, LU Shan-fu*, LIANG Da-wei,
WU Chun-xiao, XIANG Yan*
(Beijing Key Laboratory of Bio-inspired Energy Materials and Devices, School of Space and Environment, Beihang University, Beijing, 100191, *P. R. China)*

Abstract: The effect of surface modification modes on proton-over-vanadium ion selectivity was studied by spin-coating chitosan-Phosphotungstic Acid (PWA) as a single or double layer on Nafion membrane surface. To suppress the vanadium ions permeation through the Nafion® membrane in a vanadium redox flow battery (VRFB), the single surface-modified Nafion membrane (Nafion/chitosan-PWA)$_S$ and double surface-modified Nafion membrane (Nafion/chitosan-PWA)$_D$ demonstrated a 89.9% and 92.7% reduction of vanadium ion permeability in comparison with pristine Nafion, respectively. The (Nafion/chitosan-PWA)$_D$ exhibited better selectivity between proton and vanadium ions than the (Nafion/chitosan-PWA)$_S$ at the same layer thickness. Furthermore, the columbic efficiency for the VRFB single cell based on the (Nafion/chitosan-PWA)$_D$ at an optimized thickness was 93.5% and the energy efficiency was 80.7% at a charge-discharge current density of 30 mA·cm^{-2}, which were higher than the (Nafion/chitosan-PWA)$_S$ and pristine Nafion membrane. The modified membranes also possessed adequate chemical stability in the VRFB during charge-discharge cycling measurements.

Key words: surface modification mode; vanadium ion permeability; ionic selectivity; vanadium redox flow battery
CLC Number: O646 **Document Code**: A

The vanadium redox flow battery (VRFB) has attracted significant attention as an energy storage system because of its superior cycle stability, facile design and low cost[1-3]. The ion exchange membrane is used to provide separation between the anode and cathode electrolytes as well as the proton conduction in the battery[4]. The commercial Nafion® membrane has been widely studied due to its advantageous proton conductivity and chemical stability in VRFB research; however, its high vanadium permeability results in a low proton-over-vanadium ion selectivity (σ/p)[5], limiting its practical applications[6]. Thus, there has been much effort to explore ion exchange membranes with high selectivity in order to improve the cell performance of VRFB system[7-10]. A typical method is to modify Nafion membranes by introducing inorganic materials or polymers to the bulk phase or surface of Nafion[11-16].

The surface modification approach is a simple and powerful method by which a thin layer is deposited on a substrate via intermolecular forces. The surface modification of Nafion has been widely employed in the field of Direct Methanol Fuel Cells (DMFCs) to suppress methanol crossover, which include the formation of multilayered Nafion/sulfonated poly(ether ether ketone) (SPEEK)[17], layer-by-layer self-assembly of Nafion-PWA/PDDA (Poly dimethyl diallyl ammonium chloride)[18], self-assembly of Nafion/charged Au or Pd nanoparticles[19-20]. The surface-modified Nafion has also been successfully applied in

Received: 2016-03-07, Revised: 2016-04-06 *Corresponding author, Tel: (86-10)82339539, E-mail:lusf@buaa.edu.cn, xiangy@buaa.edu.cn

VRFB to improve the cell performance. For example, Qiu et al. used the polyelectrolyte layer-by-layer self-assembly technique to fabricate a barrier layer onto the surface of Nafion membrane[21]. Zeng et al. successfully prepared polypyrrole-modified Nafion membranes by electrodeposition method[22]. Luo et al. coated polyethyleneimine (PEI) on Nafion membranes via interfacial polymerization[23]. Zhang et al. prepared Nafion/SPEEK layered composite membrane via chemical crosslinking[24]. All of these modified membranes significantly suppressed the vanadium ion crossover. However, the ionic conductivity of the modified membranes drastically decreased in general, which affected the performance of the VRFB. Our recent study demonstrated that there was a significant difference between single and double surface modifications of Nafion for the methanol crossover reduction[25]. However, there are few published studies investigating the difference between single and double surface modifications of Nafion for the vanadium crossover in VRFB. Considering the porous structure and the hydrophilic sulfonic acid groups in Nafion, it is possible to block the hydrophilic channels responsible for the vanadium ion transport via intermolecular cross-linking between the sulfonic acid groups and basic groups of other polymers.

In this work, the influences of single and double surface modifications on the conductivity and vanadium crossover of Nafion membrane were investigated using representative chitosan-PWA as the modified layer. The chitosan of the modified layer is primarily utilized due to its low cost and abundant amine groups[26]. The PWA with the Keggin structure[27-28] is expected to crosslink chitosan while implemented as the proton conductor. The special surface modification modes are expected to block the vanadium ion transport channel, meanwhile to drive the proton transfer due to the introduction of PWA. Therefore, it is possible to achieve high performance of modified membranes with decreased vanadium ion permeability, comparable ionic conductivity, as well as excellent chemical stability. In addition, considering the different contact areas between Nafion surface and modified layer, it may differ in resistance effect of vanadium and proton conduction for the single and double modified membranes, and therefore, the ionic selectivity. The modified membranes together with physicochemical properties were characterized in detail. The performance and stability of the optimized single and double modified membranes were verified in VRFBs, which is considered to be a promising alternative to the commercialized Nafion.

1 Experimental

1.1 Materials

Chitosan (Aldrich-Sigma, M_w = 60,000 g·mol^{-1}) and phosphotungstic acid (Aldrich-Sigma) were used without further treatment. Ultrapure water (Millipore; 18.2 MΩ at 25 ℃), acetic acid (Aladdin Industrial Corporation, 99.5%), vanadyl sulfate ($VOSO_4$, Shenyang Haitian Fine Chemical Plant), Nafion 212 membranes were obtained from DuPont and other chemicals were purchased from commercial suppliers.

1.2 Preparation of Nafion/Chitosan –PWA Composite Membranes

There were two different modification methods on Nafion: single and double surface modifications.

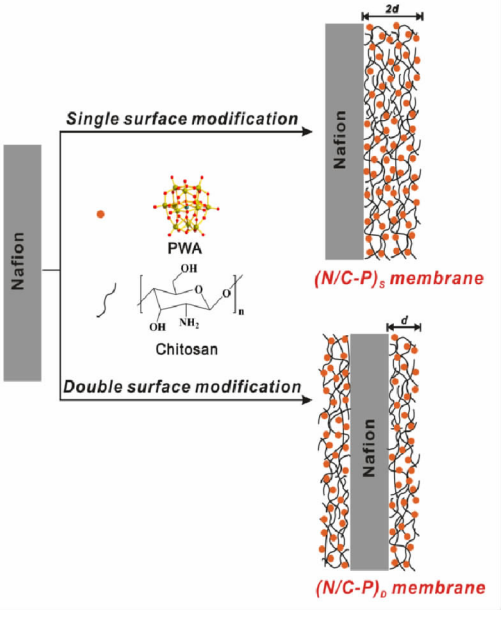

Fig. 1 The scheme of double surface modified Nafion membrane ($(N/C-P)_D$) and single surface modified Nafion membrane ($(N/C-P)_S$)

The preparation of Nafion/chitosan-PWA composite membranes, noted as $(N/C\text{-}P)_X$ (X = S or D, for single and double surface modifications, respectively), is schematically presented in Fig. 1. The Nafion 212 membrane was pretreated according to the literature[29]. The single surface modified composite membranes $(N/C\text{-}P)_S$ were prepared using a spin coater equipped with vacuum-pumping and heating system. The Nafion membrane was tightly absorbed on the suction filter area of the graphite plate placed on the hot plates at 75 ℃. Then a certain volume of 2% (by mass) chitosan solution (2 g of chitosan was dissolved in a mixture of 97 g ultrapure water and 1 g acetic acid) was spin-coated on the single side of Nafion 212 and the thickness of the thin chitosan layer was controlled by varying the volume of the chitosan solution. After this step, the Nafion/chitosan composite membrane was spin-coated by a certain amount of 5% (by mass) PWA aqueous solution at 50 ℃ and then dried at 75 ℃ to obtain the single surface Nafion/chitosan-PWA composite membrane. To prepare the double surface modified composite membranes with the same thickness as single surface modified ones, the same amount of chitosan-PWA was evenly divided and applied onto both sides of Nafion. The prepared membrane was denoted as $(N/C\text{-}P)_X$-N, where N is the thickness of the modified layer.

1.3 Membrane Characterization

The cross-sectional structures of the Nafion/chitosan-PWA composite membranes were examined by scanning electronic microscope (SEM) equipped with EDS (JEOL, JSM-5800). The infrared spectra of modified membranes were measured by FT-IR spectrometer (Thermo Fisher, USA) under the mode of attenuated total reflection. Proton conductivity was measured via electrochemical impedance spectroscopy (EIS) using Parstat 2273 advanced electrochemical workstation[30]. The water uptake of membrane were measured as reported in literature[31]. Membrane samples were immersed in the solution (1.0 mol·L^{-1} $VOSO_4$ in 3.0 mol·L^{-1} H_2SO_4) for 24 h before measuring conductivity.

The permeability measurement of VO^{2+} was carried out in a membrane-separated cell by filling 1.0 mol·L^{-1} $VOSO_4$ in one reservoir and 1.0 mol·L^{-1} $MgSO_4$ in the other reservoir to equivalent ionic strength according to the standard procedure reported[14, 32]. The osmotic concentration of VO^{2+} was detected by UV-vis spectrophotometer. The permeability of the vanadium ions was calculated via reference[32]:

$$V_B \frac{dC_B(t)}{dt} = A\frac{P}{L}(C_A\text{-}C_B(t)) \quad (1)$$

where P is the permeability of VO^{2+}, C_A is the initial VO^{2+} concentration, $C_B(t)$ refers to the VO^{2+} concentration over time, V_B is the volume of the reservoir, L and A are the thickness and cross-sectional area of the membrane, respectively.

1.4 Single Cell Test

Thd VRFB setup was assembled with two carbon felt electrodes (2 × 3 cm^2 area) fixed inside the electrode frame (thickness: 3 mm) pasted in the center of two graphite polar plates, and sandwiched between two stainless steel plates[30]. The negative and positive electrolytes (50 mL in each half-cell) consists of 1.0 mol·L^{-1} V^{2+}/V^{3+} and 1.0 mol·L^{-1} VO_2^+/VO^{2+}, both in 3.0 mol·L^{-1} H_2SO_4, respectively. The charge-discharge test was conducted with constant current mode in the voltage range of 0.8 to 1.7 V on a battery test system CT-3008-5V/1A (Neware Co., Ltd, China). Self-discharge tests were carried out by evaluating the open circuit voltage (OCV) over time after the cell was charged to an 80% state of charge (SOC) and until the OCV dropped to 0.8 V in VRFB at 20 ℃[33]. The chemical stability test was carried out by immersing several pieces of $(N/C\text{-}P)_D$-17 membranes in 1 mol·L^{-1} VO_2^+ + 3 mol·L^{-1} H_2SO_4 solution for 30 days at 20 ℃. The columbic efficiency (CE), voltage efficiency (VE), and energy efficiency (EE) of VRFB were calculated via reference[34]:

$$CE = \frac{C_d}{C_c} \times 100\% \quad (2)$$

$$VE = \frac{V_d}{V_c} \times 100\% \quad (3)$$

$$EE = \frac{E_d}{E_c} \times 100\% \quad (4)$$

where C_c and C_d are the charge and discharge capacity, respectively, V_c and V_d represent the average charge and discharge voltage, respectively.

2 Results and Discussion

2.1 FT-IR Spectroscopic Analysis

The FT-IR spectra of PWA, chitosan, Nafion 212, $(Nafion/chitosan)_D$ and $(N/C-P)_D$ membranes are shown in Fig. 2. For the Nafion 212, the characteristic peaks (980, 1057, 1149, 1207 cm^{-1}) were attributed to the vibrations of C-O-C, $-SO_3^-$, C-F and C-F in Nafion, respectively[24, 35]. Compared with the Nafion 212 membrane, the peak at 1540 cm^{-1} appeared for the $(N/C)_D$ membrane corresponded to the bending vibration of N-H bonds of chitosan ($-NH_2$). Furthermore, the peak of -NH groups in $(N/C)_D$ membrane experienced a red shift compared to pure chitosan (~ 1550 cm^{-1}), while the S-O stretching vibration of $-SO_3^-$ groups in Nafion experienced a blue shift (~ 1060 cm^{-1}), which indicates an interaction between Nafion and chitosan[28]. Furthermore, four characteristic infrared bands of $(N/C-P)_D$ membrane were observed and assigned to the stretching of $P-O_a$ bonds (1080 cm^{-1}), $W-O_d$ stretching (972 cm^{-1}), $W-O_b-W$ stretching (891 cm^{-1}) and W-Oc-W stretching (787 cm^{-1}) bands of PWA. These peaks have a red shift in comparison with those of pure PWA(1080, 980, 918, 806 cm^{-1}), respectively, which indicates that the terminal oxygen atoms of PWA strongly interact with the hydroxyl groups and the amino groups of chitosan[36]. The strong interaction between them has been confirmed by observing excess amount of insoluble complexes when chitosan and PWA solution are mixed[37-38]. The spectrum of the $(N/C-P)_S$ membrane (not shown in Fig. 2) was similar to that of $(N/C-P)_D$ membrane. All of these results indicate that the thin cross-linked chitosan-PWA layers were successfully coated on the surface of Nafion 212.

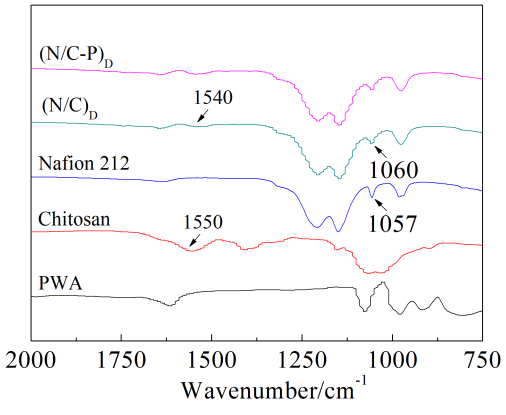

Fig. 2 FT-IR spectra of PWA, chitosan, Nafion 212, $(N/C)_D$ and $(N/C-P)_D$ membranes under the mode of attenuated total reflection

2.2 SEM and EDS Measurements

In order to further confirm the structure of the modified composite membrane, SEM images and EDS element mapping of a double surface modified Nafion were recorded. As shown in Fig. 3A, the membrane was apparently composed of three layers: Nafion layer in the center and two chitosan-PWA layers on the outer layers. The thicknesses of Nafion and each chitosan-PWA layer were about 50 μm and 8.5 μm, respectively. No delamination phenomena appeared at interfaces due to the strong adherence of electrostatic interactions between $-SO_3^-$ groups of Nafion and $-NH_3^+$ groups on chitosan chains. The EDS element mapping for the cross-section of the membrane is shown in Fig. 3B. A three-layer structure also exhibited: the fluorine element (the characteristic element of Nafion) was distributed uniformly in the center layer and the tungsten element (the characteristic element of PWA) was distributed uniformly in each modified layer, which reveals the successful modification of chitosan-PWA on the Nafion surface. Furthermore, the thickness of the modified layer was obtained from the corresponding SEM results.

2.3 Permeability of Vanadium Ions, Proton Conductivity and Selectivity

Fig. 4A compares the VO^{2+} permeabilities of $(N/C-P)_S$ and $(N/C-P)_D$ membranes with different

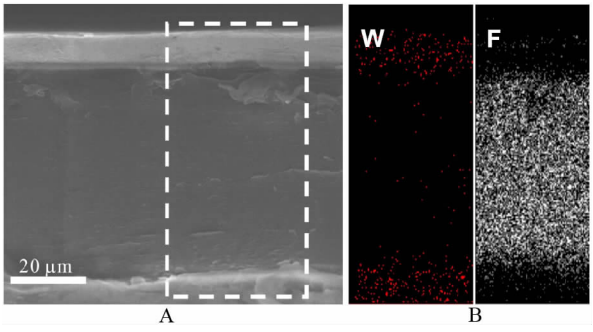

Fig. 3 A. SEM cross-section image of $(N/C-P)_D$ membrane; B. EDS cross-section image of $(N/C-P)_D$ membrane (W: wolfram; F: fluorine)

thicknesses of the modified layer. As the thickness increased from 7 to 31 μm, the permeability for both membranes (single and double surface modified Nafion) quickly decreased. In particular, the permeability lowered apparently with the thickness of chitosan-PWA layer increased from 7 to 17 μm and then remained constant as the thickness of the modified layer further increased from 17 to 31 μm, indicating that the modified layer reached their limit to block the vanadium ions crossover with the thickness of 17 μm. And the permeability of VO^{2+} ion decreased to 1.19×10^{-7} $cm^2 \cdot min^{-1}$ for $(N/C\text{-}P)_S$-17 membrane and 1.10×10^{-7} $cm^2 \cdot min^{-1}$ for $(N/C\text{-}P)_D$-17 membrane, exhibiting 89.9% and 90.6% reductions, respectively, compared with that of 11.74×10^{-7} $cm^2 \cdot min^{-1}$ for pristine Nafion membrane. The high permeability of vanadium ions through Nafion membrane could be attributed to the hydrophilic channels formed with polar clusters of $-SO_3^-$ groups which could allow the transport of both protons and vanadium ions. The effective reduction of vanadium ions permeability was mainly caused by the blocking of hydrophilic channels of Nafion membranes due to the electrostatic interaction between the negatively charged $-SO_3^-$ groups in Nafion and positively charged $-NH_3^+$ groups in chitosan[22, 39]. Meanwhile, the electrostatic repulsion between the positively charged chitosan and vanadium ions may be another important reason for the decreased vanadium ions permeability. However, the hydrophilic channels could only be partially blocked when the thickness of the modified layer was less 17 μm, which resulted in the obvious difference in vanadium ions permeability as shown in Fig. 4A. As the thickness of the modified layer increased to 25 or 31 μm, the blocking to hydrophilic channels reached a limit, therefore, the vanadium ions permeability only changed slightly. The porous spike-like structure of the chitosan-PWA layer studied in our previous work[18, 27] might be the reason for the almost unchanged vanadium ions permeability of the as-prepared membranes as the modification layer thickness increased above 25 or 31 μm. With the same modified layer thickness, the vanadium ions permeability of the $(N/C\text{-}P)_D$ membranes was lower than that of $(N/C\text{-}P)_S$ membranes mainly due to the contact area between Nafion membrane and modified layers, where the entrance of hydrophilic channels for vanadium ions crossover in Nafion was inhibited much more seriously for the $(N/C\text{-}P)_D$ membranes.

The proton conductivities (σ) of Nafion membranes with different thicknesses of single or double modified layers are shown in Fig. 4B. It is clear that the σ values of both $(N/C\text{-}P)_D$ and $(N/C\text{-}P)_S$ membranes gradually decreased with an increase in thickness of chitosan-PWA layer from 7 to 31 μm. However, the σ values of the $(N/C\text{-}P)_D$ membrane showed a slight decrease with increased thickness of chitosan-PWA layer from 7 to 17 μm, which is much better than that of the $(N/C\text{-}P)_S$ membrane with the same modified layer thickness. Especially, the proton conductivity (1.23×10^{-2} $S \cdot cm^{-1}$) of $(N/C\text{-}P)_D$-17 was 1.7 times larger than that of $(N/C\text{-}P)_S$-17 (0.72×10^{-2} $S \cdot cm^{-1}$), and the differences increased to 2.4 times larger for thickness of 31 μm. In the electrolyte of VRFB, H_2SO_4 was used as the supported electrolyte for the proton transport. The chitosan-PWA layer would block the transport of proton and therefore the proton conductivity decreased after the modification. Based on the fact that the proton conductivities of $(N/C\text{-}P)_S$-7 and $(N/C\text{-}P)_D$-17 were almost the same, a modification layer with the thickness less than 7 ~ 9 μm would allow the free transport of proton in H_2SO_4 electrolyte. Since the proton conductivity is related with the water uptake, the measured water uptake values of 28.1%, 22.4%, 21.9% and 21.6% were recorded for Nafion 212, $(N/C\text{-}P)_D$-7, $(N/C\text{-}P)_D$-12 and $(N/C\text{-}P)_D$-17 membranes, respectively. These results well agreeed with their proton conductivities trends in Fig. 4B.

An ideal ion exchange membrane in a VRFB should possess both low vanadium ion permeability and high ionic conductivity. Thus, the selectivity is more reasonable to evaluate the comprehensive performance including the practical application. The selectivity (proton conductivity over vanadium permeability) curves of the Nafion with different modification modes are presented in Fig. 4C. The results

demonstrate that both single and double modified membranes exhibited larger selectivity than Nafion, and the double modified membranes were even better than single layered membranes at all thicknesses. Furthermore, the maximum selectivity occurs at the modification layer thickness of 17 μm for both single and double modified membranes. In particular, the selectivities of $(N/C\text{-}P)_S$-17 and $(N/C\text{-}P)_D$-17 membranes were 6.16 ×10^4 and 1.12 × 10^5 S·min·cm^{-3}, which were 4.5 and 8.3 times higher, respectively, than that of pristine Nafion membrane (1.35 × 10^4 S·min·cm^{-3}). As a result, the optimized membranes, $(N/C\text{-}P)_D$-17 and $(N/C\text{-}P)_S$-17, were utilized in the sub-subsequent tests for VRFB single cell performance.

2.4 VRFB Single Cell Performance

The charge-discharge curves of VRFB, incorporating Nafion, $(N/C\text{-}P)_S$-17 or $(N/C\text{-}P)_D$-17 membranes at a current density of 30 mA·cm^{-2} to 60 mA·cm^{-2}, are presented in Fig. 5. It can be found that the charge and discharge platforms of the VRFB with $(N/C\text{-}P)_D$-17 were better relative to that of $(N/C\text{-}P)_S$-17, while the discharge platforms of both VRFB with $(N/C\text{-}P)_D$-17 and $(N/C\text{-}P)_S$-17 were slightly poor relative to the Nafion device. This result might be attributed to the higher area resistance of the modified membranes. Furthermore, the discharge specific capacity of VRFB with $(N/C\text{-}P)_D$-17 was higher than that with $(N/C\text{-}P)_S$-17 or Nafion due to the highest selectivity of the $(N/C\text{-}P)_D$-17 membrane.

The Coulombic efficiency (*CE*), voltage efficiency (*VE*) and energy efficiency (*EE*) plots of the VRFB under different charge/discharge current densities are shown in Fig. 6. The *CE* of the VRFB based on the three membranes increased with a larger current density, while the *VE* of the VRFB exhibited an opposite trend. This could be attributed to the shorter time for vanadium crossover and the enhanced ohmic polarization together with the over-potentials[40]. The VRFB with $(N/C\text{-}P)_D$-17 showed higher *CE*, *VE* and *EE* than those of $(N/C\text{-}P)_S$-17 or Nafion membrane at all current densities, in good agreement with the VO^{2+} permeability and ionic conductivity results in Fig. 4. Especially, the VRFB with $(N/C\text{-}P)_D$-17 presented a *CE*

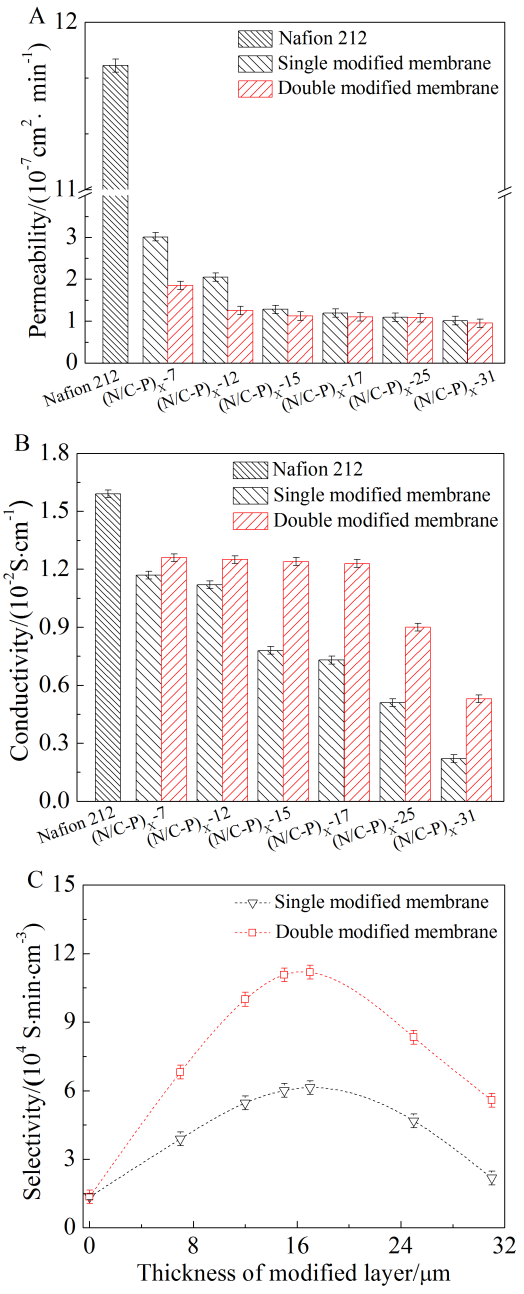

Fig. 4 A. The vanadium ion permeabilities of Nafion 212, $(N/C\text{-}P)_S$ and $(N/C\text{-}P)_D$ membranes; B. The proton conductivities of Nafion 212, $(N/C\text{-}P)_S$ and $(N/C\text{-}P)_D$ membranes (tested at 20 ℃ under dry air); C. The selectivities of the $(N/C\text{-}P)_S$ and $(N/C\text{-}P)_D$ membranes with different thicknesses of the modified layer

of 93.4% ~ 96.2% when the current density increased from 30 to 80 mA·cm^{-2}, while the *CE* of VRFB with Nafion increased from 80.1% to 94.3%. However, due to the vanadium ion crossover and increased ohmic polarization loss of the VRFB, the *VE* and *EE*

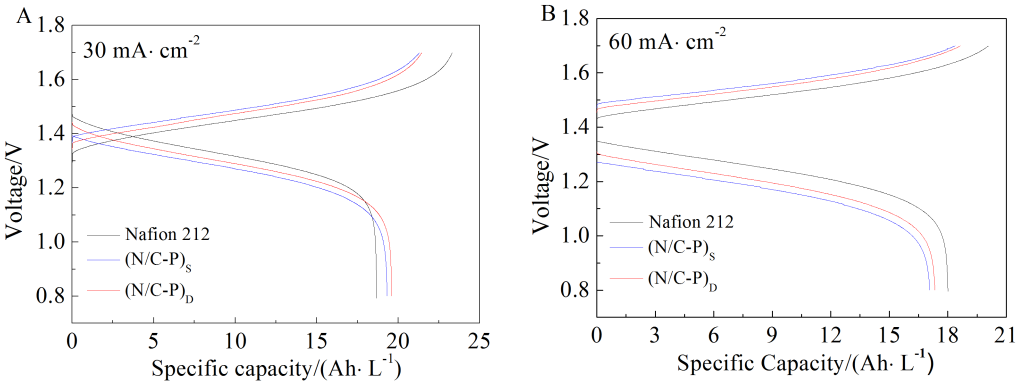

Fig. 5 Charge/discharge curves of VRFB assembled with Nafion 212, $(N/C-P)_S$ and $(N/C-P)_D$ membranes, respectively, at 30 mA·cm^{-2} (A) and 60 mA·cm^{-2} (B)

were decreased under larger current densities. In addition, the VRFB with $(N/C-P)_D$-17 exhibited the maximum *EE* of 80.7% compared with those of 77.9% and 73.6% for the cell with $(N/C-P)_S$-17 and Nafion, respectively, at a current density of 30 mA·cm^{-2}.

The self-discharge rates of VRFB with the different membranes could be evaluated by the OCV after an elapsed amount of time. As shown in Fig. 7A, initially, the OCV value slowly decreased and then rapidly decreased to 0.8 V. For the VRFB with $(N/C-P)_D$-17 or $(N/C-P)_S$-17 membrane, the time for OCV value that maintainsed above 0.8 V were about 93 h and 86 h, respectively, which was significantly longer than that of VRFB with Nafion (59 h). The result was in accordance with the vanadium ion permeability data that suggested self-discharge rate of VRFB with the $(N/C-P)_D$-17 being lower than that of VRFB with $(N/C-P)_S$-17 or Nafion[41].

To evaluate the stability of the modified membrane under practical working conditions of a VRFB, the charge-discharge cycling test of the VRFB was performed. Fig. s 7B and 7C show that the *CE* and *EE* curves of the VRFB cell assembled with the modified membrane displayed no obvious attenuation over 30 cycles, which indicates that both $(N/C-P)_S$-17 and $(N/C-P)_D$-17 membranes possessed good stability in vanadium solutions. Moreover, the *CE* and *EE* plots of VRFB with $(N/C-P)_D$-17 membrane always remained higher than that with the $(N/C-P)_S$-17 membrane during the 30-cycle measurement. The discharge ca-

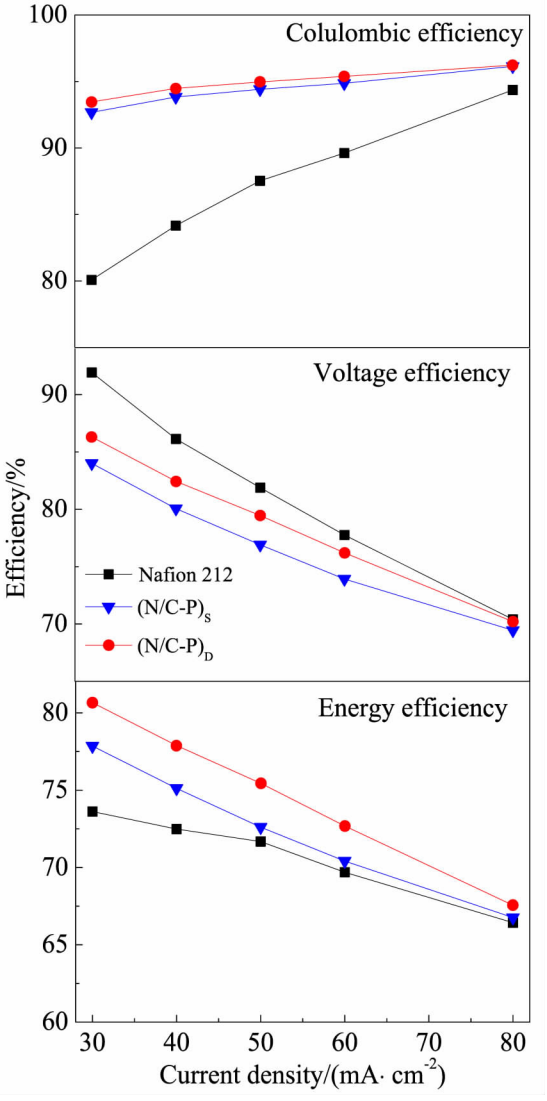

Fig. 6 Effects of charge/discharge current density on *CE* (top), *VE* (middle) and *EE* (bottom) of the VRFB with Nafion 212, $(N/C-P)_S$ and $(N/C-P)_D$ membranes, respectively.

pacities of the VRFB based on$(N/C\text{-}P)_X$-17 and Nafion are presented in Fig. 7D. During the 30 cycles, the capacity of the VRFB with the $(N/C\text{-}P)_D$-17 membrane exhibited the smallest deterioration, while the capacity of the cell with Nafion clearly decayed. After 30 cycles, the capacities of the VRFB based on $(N/C\text{-}P)_D$-17, $(N/C\text{-}P)_S$-17 and Nafion membranes were maintained at 92%, 88% and 86% of their initial capacities, respectively. Obviously, the VRFB assembled with the $(N/C\text{-}P)_D$-17 membrane showed much better capacity stability than that with Nafion. This might be mainly ascribed to the different selective permeabilities caused by crossover of vanadium ions through the membranes during the charge-discharge cycling of the battery.

To further investigate the long-time chemical stability of the modified membranes in vanadium electrolyte, the VRFB assembled with $(N/C\text{-}P)_D$-17 was cycled under a current density of 60 mA·cm^{-2}. As illustrated in Fig. 8A, there was no obvious efficiency decline within 200 cycling test. The thickness of each chitosan-PWA layer coated on Nafion was measured to be about 8 μm and no delamination phenomenon appeared at the interfaces, which could be well reflected by the cross-section EDS mapping of soaked $(N/C\text{-}P)_D$-17 (Fig. 8B). In addition, no obvious defect was observed[42] on the surface of the soaked $(N/C\text{-}P)_D$-17 membrane (Fig. 8C), and the vanadium ions permeability (1.20×10^{-7} cm^2·min^{-1}) of the $(N/C\text{-}P)_D$-17 membrane after 200 cycling test was relatively unchanged compared to the initial value (1.10×10^{-7} cm^2·min^{-1}). Based on these results, the chemical stability of the typical $(N/C\text{-}P)_D$-17 membrane was verified, which in turn supported the research theme of this work.

3 Conclusions

The proton conductivity and vanadium ions permeability of the surface modified Nafion with single

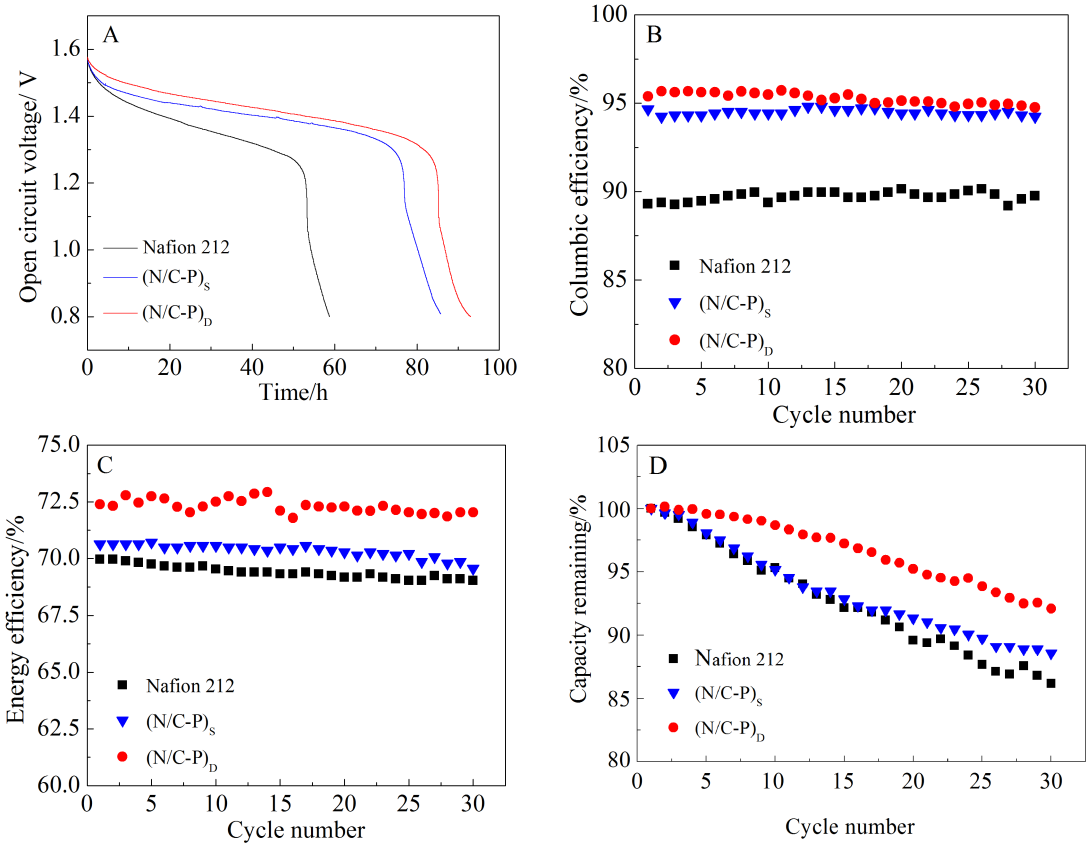

Fig. 7 A. OCV curves displaying VRFB single cells with Nafion 212, $(N/C\text{-}P)_S$ and $(N/C\text{-}P)_D$ membranes at SOC = 80%; B-C. cycling effects on CE and EE data for the VRFB with Nafion 212, $(N/C\text{-}P)_S$ and $(N/C\text{-}P)_D$ membranes at a current density of 60 mA·cm^{-2}; D. normalized discharge capacity of the VRFB as a function of cycle number at 60 mA·cm^{-2}

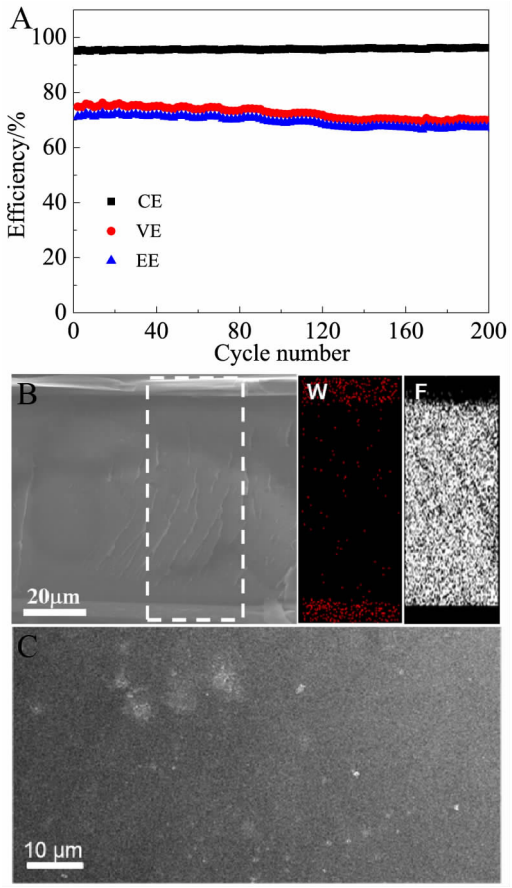

Fig. 8 A. Cycling performance of VRFB assembled with $(N/C\text{-}P)_D$-17 membrane at a current density of 60 mA·cm^{-2}; B-C. The SEM and EDS cross-sectional images of the $(N/C\text{-}P)_D$-17 and SEM surface image of the $(N/C\text{-}P)_D$-17 membrane after soaked in vanadium salt solutions for 30 days

or double chitosan-PWA layers to form composite membranes were studied. The performance and stability of the VRFB cells assembled with the composite membranes were also investigated and compared with those unmodified Nafion membrane 212. The $(N/C\text{-}P)_D$-17 and $(N/C\text{-}P)_S$-17 membranes had significantly lowered the permeability of vanadium ions than Nafion 212, resulting in the longer self-discharge duration of the VRFB (93 h with $(N/C\text{-}P)_D$-17 and 86 h with $(N/C\text{-}P)_S$-17), which were about 1.6 and 1.4 times, respectively, longer than that of VRFB with Nafion 212 (59 h). The double surface modified membranes exhibited a higher selectivity than the single surface modified membranes with the same modified layer thickness. As a result, the VRFB single cell assembled with $(N/C\text{-}P)_D$-17 showed higher Coulombic efficiency and energy efficiency at current densities ranging from 30 to 80 mA·cm^{-2}, while the VRFB with the $(N/C\text{-}P)_D$-17 membrane exhibited a lower degradation rate in discharge capacity at the current density of 60 mA·cm^{-2} compared to that with $(N/C\text{-}P)_S$-17 or unmodified Nafion. At 30 mA·cm^{-2}, the energy efficiency of 80.7% was achieved with the $(N/C\text{-}P)_D$-17 membrane, which was larger than those with $(N/C\text{-}P)_S$-17 (77.9%) and Nafion 212 (73.6%). The adequate chemical and capacity stabilities were also oberved from the cycling test. This surface modification mode offers a direction for the advancement of proton exchange membranes applied in VRFBs and is valuable in solving the electrolyte penetration dilemma.

Acknowledgement

This work was financially supported by grants from the National Natural Science Foundation of China (No. 51422301), Beijing Higher Education Young Elite Teacher Project (No. 29201493) and the Fundamental Research Funds for the Central Universities(No.YWF-16-BJ-Y-68).

References:

[1] Sum E, Rychcik M, Skyllas-Kazacos M. Investigation of the V(V)/V(IV) system for use in the positive half-cell of a redox battery[J]. Journal of Power Sources, 1985, 16(2): 85-95.

[2] Xu Q, Zhao T S, Leung P K. Numerical investigations of flow field designs for vanadium redox flow batteries [J]. Applied Energy, 2013, 105: 47-56.

[3] Zhang C, Zhao T S, Xu Q, et al. Effects of operating temperature on the performance of vanadium redox flow batteries[J]. Applied Energy, 2015, 155: 349-353.

[4] Wang W, Luo Q T, Li B, et al. Recent progress in redox flow battery research and development[J]. Advanced Functional Materials, 2013, 23(8): 970-986.

[5] Shen J, Xi J Y, Zhu W T, et al. A nanocomposite proton exchange membrane based on PVDF, poly (2-acrylamido-2-methyl propylene sulfonic acid), and nano-Al_2O_3 for direct methanol fuel cells[J]. Journal of Power Sources, 2006, 159(2): 894-899.

[6] Li X F, Zhang H M, Mai Z S, et al. Ion exchange membranes for vanadium redox flow battery (VRB) applications[J]. Energy & Environmental Science, 2011, 4(4): 1147-1160.

[7] Xi J Y, Wu Z H, Qiu X P, et al. Nafion/SiO_2 hybrid mem brane for vanadium redox flow battery[J]. Journal of Power Sources, 2007, 166(2): 531-536.

[8] Wang Z, Tang H L, Zhang H J, et al. Synthesis of Nafion/CeO_2 hybrid for chemically durable proton exchange membrane of fuel cell[J]. Journal of Membrane Science, 2012, 421: 201-210.

[9] Teng X G, Zhao Y T, Xi J Y, et al. Nafion/organic silica modified TiO_2 composite membrane for vanadium redox flow battery via *in situ* sol-gel reactions[J]. Journal of Membrane Science, 2009, 341(1): 149-154.

[10] Teng X G, Zhao Y T, Xi J Y, et al. Nafion/organically modified silicate hybrids membrane for vanadium redox flow battery[J]. Journal of Power Sources, 2009, 189(2): 1240-1246.

[11] Mai Z S, Zhang H M, Li X F, et al. Nafion/polyvinylidene fluoride blend membranes with improved ion selectivity for vanadium redox flow battery application[J]. Journal of Power Sources, 2011, 196(13): 5737-5741.

[12] Jie Z, Tang H L, Mu P. Fabrication and characterization of self-assembled Nafion-SiO_2-ePTFE composite membrane of PEM fuel cell[J]. Journal of Membrane Science, 2008, 312(1): 41-47.

[13] Teng X G, Dai J C, Su J, et al. A high performance polytetrafluoroethene/Nafion composite membrane for vanadium redox flow battery application[J]. Journal of Power Sources, 2013, 240: 131-139.

[14] Wang N F, Peng S, Lu D, et al. Nafion/TiO_2 hybrid membrane fabricated via hydrothermal method for vanadium redox battery[J]. Journal of Solid State Electrochemistry, 2012, 16(4): 1577-1584.

[15] Kim Jihoon, Jeon Jae-Deok, Kwak Seung-Yeop. Nafion-based composite membrane with a permselective layered silicate layer for vanadium redox flow battery[J]. Electrochemistry Communications, 2014, 38:68-70.

[16] Teng X G, Dai J C, Su J, et al. Modification of Nafion membrane using fluorocarbon surfactant for all vanadium redox flow battery[J]. Journal of Membrane Science, 2015, 476: 20-29.

[17] Yang B, Manthiram A. Multilayered membranes with suppressed fuel crossover for direct methanol fuel cells[J]. Electrochemistry Communications, 2004, 6 (3): 231-236.

[18] Yang M, Lu S F, Lu J L, et al. Layer-by-layer self-assembly of PDDA/PWA-Nafion composite membranes for direct methanol fuel cells[J]. Chemical Communications, 2010, 46(9): 1434-1436.

[19] Mu S C, Tang H L, Wan Z H, et al. Au nanoparticles self-assembled ont o Nafion membranes for use as methanol-blocking barriers[J]. Electrochemistry Communications, 2005, 7(11): 1143-1147.

[20] Tang H L, Pan M, Jiang S P, et al. Self-assembling multi-layer Pd nanoparticles onto Nafion® membrane to reduce methanol crossover[J]. Colloids and Surfaces A: Physicochemical and Engineering Aspects, 2005, 262 (1): 65-70.

[21] Xi J Y, Wu Z H, Teng X G, et al. Self-assembled polyelectrolyte multilayer modified Nafion membrane with suppressed vanadium ion crossover for vanadium redox flow batteries[J]. Journal of Materials Chemistry, 2008, 18 (11): 1232-1238.

[22] Zeng J, Jiang C P, Wang Y H, et al. Studies on polypyrrole modified nafion membrane for vanadium redox flow battery[J]. Electrochemistry Communications, 2008, 10 (3): 372-375.

[23] Luo Q T, Zhang H M, Chen J, et al. Modification of Nafion membrane using interfacial polymerization for vanadium redox flow battery applications[J]. Journal of Membrane Science, 2008, 311(1): 98-103.

[24] Luo Q T, Zhang H M, Chen J, et al. Preparation and characterization of Nafion/SPEEK layered composite membrane and its application in vanadium redox flow battery [J]. Journal of Membrane Science, 2008, 325(2): 553-558.

[25] Xiang Y, Zhang J, Liu Y, et al. Design of an effective methanol-blocking membrane with purple membrane for direct methanol fuel cells[J]. Journal of Membrane Science, 2011, 367(1): 325-331.

[26] Mengatto L, Luna J A, Cabrera M I. Influence of cross-linking density on swelling and estradiol permeation of chitosan membranes[J]. Journal of Materials Science, 2010, 45(4): 1046-1051.

[27] Lu S F, Wu C X, Liang D W, et al. Layer-by-layer self-assembly of Nafion-[CS-PWA] composite membranes with suppressed vanadium ion crossover for vanadium redox flow battery applications[J]. RSC Advances, 2014, 4(47): 24831-24837.

[28] Lu J L, Tang H L, Lu S F, et al. A novel inorganic proton exchange membrane based on self-assembled HPW-meso-silica for direct methanol fuel cells[J]. Journal of Materials Chemistry, 2011, 21(18): 6668-6676.

[29] Jiang S P, Liu Z C, Tian Z Q. Layer-by-layer self-assembly of composite polyelectrolyte-nafion membranes for direct methanol fuel cells[J]. Advanced Materials, 2006, 18(8): 1068-1072.

[30] Zhang F X, Zhang H M, Qu C. A dication cross-linked composite anion-exchange membrane for all-vanadium flow battery applications[J]. ChemSusChem, 2013, 6(12):

2290-2298.

[31] Pan J, Lu S F, Li Y, et al. High-performance alkaline polymer electrolyte for fuel cell applications[J]. Advanced Functional Materials, 2010, 20(2): 312-319.

[32] Luo X L, Lu Z Z, Xi J Y, et al. Influences of permeation of vanadium ions through PVDF-g-PSSA membranes on performances of vanadium redox flow batteries[J]. The Journal of Physical Chemistry B, 2005, 109(43): 20310-20314.

[33] Teng X G, Dai J C, Bi F Y, et al. Ultra-thin polytetrafluoroethene/Nafion/silica composite membrane with high performance for vanadium redox flow battery[J]. Journal of Power Sources, 2014, 272:113-120.

[34] Chen D Y, Hickner M A, Agar E, et al. Optimized anion exchange membranes for vanadium redox flow batter ies[J]. ACS Applied Materials &Interfaces, 2013, 5(15): 7559-7566.

[35] Cui Z L, Drioli E, Lee Y M. Recent progress in fluoropolymers for membranes[J]. Progress in Polymer Science, 2014, 39(1): 164-198.

[36] Hsu W Y, Gierke T D. Ion transport and clustering in Nafion perfluorinated membranes[J]. Journal of Membrane Science, 1983, 13(3): 307-326.

[37] Cui Z M, Xing W, Liu C P, et al. Chitosan/heteropolyacid composite membranes for direct methanol fuel cell[J]. Journal of Power Sources, 2009, 188(1): 24-29.

[38] Shakeri S E, Ghaffarian S R, Tohidian M, et al. Polyelectrolyte nanocomposite membranes, based on chitosan-phosphotungstic acid complex and montmorillonite for fuel cells applications[J]. Journal of Macromolecular Science, Part B, 2013, 52(9): 1226-1241.

[39] Jae D J, Seung Y K. Ionic cluster size distributions of swollen Nafion/sulfated beta-cyclodextrin membranes characterized by nuclear magnetic resonance cryoporometry[J]. Journal of Physical Chemistry B, 2007, 111(32): 9437-9443.

[40] Zhang B G, Zhang E L, Wang G S, et al. Poly (phenyl sulfone) anion exchange membranes with pyridinium groups for vanadium redox flow battery applications[J]. Journal of Power Sources, 2015, 282:328-334.

[41] Mai Z S, Zhang H M, Zhang H Z, et al. Anion-conductive membranes with ultralow vanadium permeability and excellent performance in vanadium flow batteries[J]. ChemsusChem, 2013, 6(2): 328-335.

[42] Xu W X, Zhao Y Y, Yuan Z Z, et al. Highly stable anion exchange membranes with internal cross-linking networks[J]. Advanced Functional Materials, 2015, 25(17): 2583-2589.

表面修饰模式对 Nafion 离子选择性影响及在 VRFB 中的应用

谭青龙,王海宁,卢善富*,梁大为,武春晓,相　艳*

(北京航空航天大学空间与环境学院, 仿生能源材料与器件北京市重点实验室, 北京, 100191)

摘要: 本文采用壳聚糖-磷钨酸层对 Nafion 膜表面分别进行单面和双面修饰改性,研究了修饰模式对 Nafion 膜钒离子渗透率、电导率及离子选择性的影响. 结果表明,单面、双面修饰改性均会使 Nafion 膜的钒离子渗透率显著降低,最高降幅分别达到 89.9%(单面修饰)和 92.7%(双面修饰);单面、双面修饰改性均会使 Nafion 膜的电导率下降,但存在明显差异,在相同修饰厚度条件下,双面修饰改性对 Nafion 膜电导率的影响比单面修饰改性更小. 因此,双面修饰复合膜展示出了比单面修饰复合膜更高的离子选择性,并且在修饰层厚度为 17 μm 时达到最大值(1.12×10^5 S·min·cm^{-3}). 基于优化的双面修饰 Nafion 膜的全钒液流电池,在充放电流密度 30 mA·cm^{-2} 时,库仑效率和能量效率分别达到 93.5%和 80.7%,并在测试时间内展示出良好的循环稳定性.

关键词: 表面修饰模式; 钒离子渗透率; 离子选择性; 全钒液流电池